# Subsequent Commutation Failure Suppression Method Based on Optimized Current Error Controller Parameters

Zhixian Li
*State Key Laboratory of Alternate Electrical Power System with Renewable Energy Sources*
*North China Electric Power University*
Beijing, China
lizhixian777@163.com

Chongru Liu
*State Key Laboratory of Alternate Electrical Power System with Renewable Energy Sources*
*North China Electric Power University*
Beijing, China
chongru.liu@ncepu.edu.cn

You Zuo
*State Key Laboratory of Alternate Electrical Power System with Renewable Energy Sources*
*North China Electric Power University*
Beijing, China
you_zuo1223@163.com

Yibo Shi
*State Key Laboratory of Alternate Electrical Power System with Renewable Energy Sources*
*North China Electric Power University*
Beijing, China
shi_yb_prc@qq.com

2022 4th International Conference on Smart Power & Internet Energy Systems (SPIES) | 978-1-6654-8957-7/22/$31.00 ©2022 IEEE | DOI: 10.1109/SPIES55999.2022.10082040

***Abstract*—In order to improve the ability of the HVDC transmission system to resist subsequent commutation failure, subsequent commutation failure suppression method based on optimized current error controller parameters is proposed. Firstly, the mechanism of the effect of the extinction angle increment of the current error controller output on the subsequent commutation failure is analyzed. Besides, the slope of current error controller (CEC) is optimized offline by using deep reinforcement learning, leading to the proposed CEC control method of adaptive slope with offline optimization and online simulation. Finally, the effectiveness of the proposed suppression strategy is verified by using the CIGRE standard test model.**

***Keywords*—HVDC, subsequent commutation failure, commutation capability index, current error controller**

## I. INTRODUCTION

Line commutated converter high voltage direct current (LCC-HVDC) is a major component of the hybrid AC-DC grid [1], however, the use of thyristor as a commutation element has the risk of commutation failure in LCC-HVDC systems [2]. With the increasingly close coupling between AC-DC systems, the impact of faults on grid operation is shifting from local to global. Simulations show that the system can withstand about twice commutation failures of a single UHVDC system without taking measures, and multiple commutation failures bring about DC power dropping and other problems that may beyond the tolerance of the system [3]. Therefore, it is of great significance to study the mechanism and influencing factors of the subsequent commutation failure and propose corresponding suppression measures for safe and reliable operation of power grid in our country.

Existing studies show that the main cause of subsequent commutation failure is improper interaction of the inverter controller [4], so most of the studies propose corresponding improvement measures from the perspective of DC control systems. In the literature [5], starting from the current error controller (CEC) in the DC system, a control strategy that can dynamically adjust the constant extinction angle increment according to the severity of the AC fault is proposed, thus improving the immunity to subsequent commutation failures. The literature [6] adjusts the upper limit of the constant extinction angle increment and the starting voltage rectification value based on the literature [5] to enhance the DC transmission power during faults. The literature [7] proposes a method for adaptively adjusting the slope of the current deviation control in response to the changing system state.

However, the current error controller (CEC) parameters are relatively unreasonable in existing studies, for recent CEC parameters debugging work still depends on aimless simulation experiments. Therefore, this paper proposes a CEC slope optimization method based on deep reinforcement learning. Firstly, the mechanism of the effect of inverter control mode switching on the subsequent commutate failure is analyzed, then a controller is designed to increase the CEC slope which can accelerate the control switching on the inverter side. Subsequently, a convolutional neural network (CNN) is used to extract information about the power system environment, which is combined with a deep Q network (DQN) to form a deep reinforcement learning-based control parameter optimization model, and the trained model is used to optimize the slope of the controller ramp function, thus achieving the purpose of suppressing the subsequent commutate failures.

## II. MECHANISTIC ANALYSIS

During the fault recovery process, the inverter AC bus voltage amplitude is still at the fault level, and the continuous rebound of DC may cause subsequent commutate failures in the DC system. At this point, the inverter control is in constant current (CC) control mode, and the CEC fails, so the CEA tends to fall uncontrollably, further leading to subsequent commutate failure. In order to illustrate the above process more clearly, the following mainly use the CIGRE HVDC model as typical simulation cases to analyze above procession. A three-phase short circuit occurring at 2.0s is set at the inverter converter bus, the ground inductance $L_f$ is 0.8H, and the fault is cleared after 0.5s. Fig. 1 is a block diagram of the DC control system in CIGRE HVDC model, where $U_d$ is the DC voltage on the inverter side, $I_{co}$ is the manual input current value, $I_d$ is the DC current on the inverter side, $\gamma_{min}$ is the minimum constant extinction angle of the upper and lower bridge arms of the inverter, $I_{dref}$ is the DC current order value, $\Delta\gamma$ is the constant extinction angle error, $\beta_C$ is the constant current control advanced trigger angle, and $\beta_G$ is the constant extinction angle (CEA) control advanced trigger angle, $\alpha_i$ is the trigger angle of the inverter.

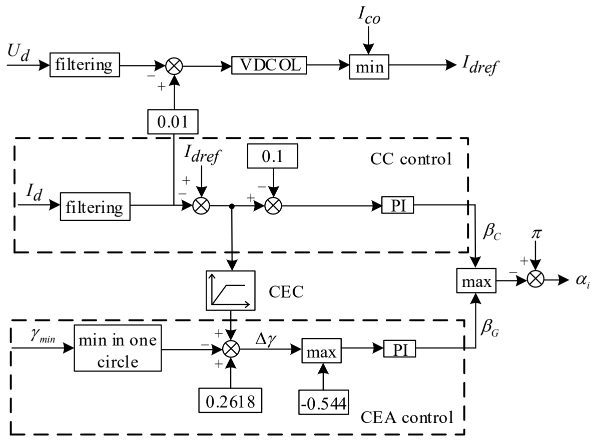


Fig. 1. Structure of DC control system

After the first commutation failure, both the DC current and the DC voltage tend to the zero axis due to the overshoot phenomenon of the PI controller, and the control response characteristics of the DC system after the fault are shown in Fig. 2.

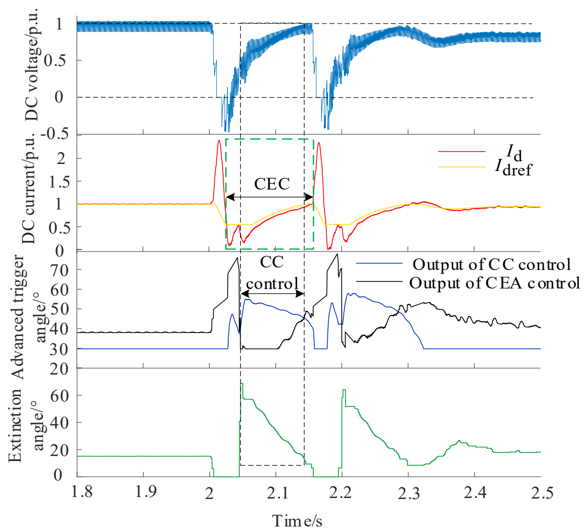


Fig. 2. DC control response characteristics after fault

As shown in the figure above, the start of the CEC is switched in advance of the mode switching on the inverter. When the DC current is less than the command value, the DC system quickly increases the advanced trigger angle $\beta_G$ output by the CEA controller through CEC, so as to achieve the purpose of quickly increasing the value of the CEA. At this time, the CEA has been raised to a larger value, and the demand for pullbacks is obvious, so the $\beta_G$ will drop rapidly to adjust the size of the CEA. When $\beta_G$ is equal to the output of the advance trigger angle $\beta_C$, the inverter control mode will switch to CC control. At this stage, the direct voltage is in the recovery period of the slope, and the DC current will gradually recover. When the commutation voltage is at the fault level, the slight change of the direct current can also lead to commutation failure, so this stage especially requires the coordination of the inverter control to accelerate the switching of the inverter control mode.

## III. CEC Slope Optimization Method Based on Deep Reinforcement Learning

### A. CEC Characterization

The characteristic curve of the CEC is shown in Fig. 3.

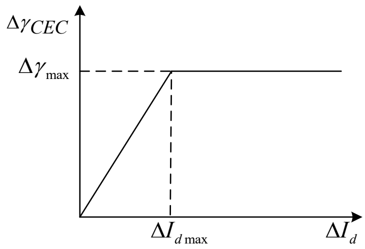


Fig. 3. CEC characteristic curve

where $\Delta I_d$ is the current error, $\Delta I_{d\max}$ is the maximum current error, $\Delta\gamma_{CEC}$ is the CEA increment of the CEC output, and $\Delta\gamma_{\max}$ is the maximum value of the CEA increment. $\Delta I_d$ is expressed as:

$$\Delta I_d = I_{dref} - I_d \tag{1}$$

In the CIGRE HVDC model, $\Delta\gamma_{CEC}$ is expressed as:

$$\Delta\gamma_{CEC} = \begin{cases} 16^{\circ} & \Delta I_d \geq 0.1 \\ 160\Delta I_{d\max} & 0 \leq \Delta I_d < 0.1 \end{cases} \tag{2}$$

In Figure 1, the CEA-controlled extinction angle error $\Delta\gamma$ enters the PI controller after the limit session, and $\Delta\gamma$ can be expressed as:

$$\Delta\gamma = \Delta\gamma_{CEC} + \gamma_{ref} - \gamma \tag{3}$$

When the inverter is in the CC control mode, the CEA gradually returns to the reference value, and the proportion of $\Delta\gamma_{CEC}$ in $\Delta\gamma$ gradually increases, and $\Delta\gamma_{CEC}$ plays a key role in the switching of the control mode of the inverter. Therefore, it can be considered to increase the slope of CEC in the inverter CC control mode and increase the output of the CEA increment, thereby accelerating the switching of the inverter control mode.

### B. Deep Reinforcement Learning Optimizes CEC Slope

In this paper, the CIGRE standard model is used to verify the effect of the control strategy on subsequent commutation failures, and the main equipment system structure of CIGRE HVDC diagram is shown in Fig. 4 [8-9].

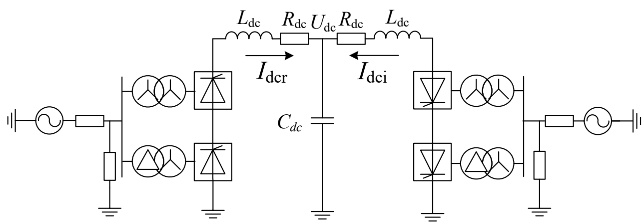


Fig. 4. Main equipment system structure of CIGRE HVDC

In the figure, $L_{dc}$, $C_{dc}$, and $R_{dc}$ are the inductance, capacitance and resistance of the DC line, respectively; $U_{dc}$ is the DC line midpoint capacitance voltage; $I_{dcr}$ and $I_{dci}$ are direct currents on the rectifier side and inverter side, respectively.

Using CIGRE HVDC standard system as test system, the model input data is the amplitude of the AC bus voltage drop on the inverter and the reactive power injected into DC system. The following is a typical policy case as an example to illustrate the training process. By changing the voltage of the voltage source at both ends to obtain samples under different operating states of the system, setting the three-phase short circuit to occur at the inverter busbar in 2.0s, the fault duration is 0.5s, and the fault ground inductance is 0.8H, and the CEC session is rewritten into a parameter visualization module, as shown in the following figure:

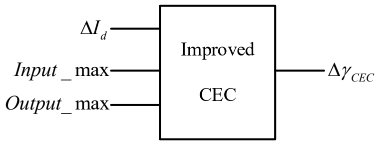


Fig. 5. Customized module of improved CEC

In the CIGRE HVDC model, the input_max takes 0.1 and the Output_max takes 0.2793 to avoid difficulties in training the model due to excessive action space. Through simulation, the optimal range of input_max is 0.03 to 0.15, and the optimal range of output_max is 0.20 to 0.35. Both parameters have a regulation step of 0.01.

Because the CEA margin during fault recovery needs to be large enough to enhance the ability of the DC system to resist subsequent commutation failures, the reward function $r$ is set as follows

$$r = \begin{cases} \lambda, & \gamma_{\min} < 7.2 \\ \mu(\gamma_{\min} - 7.2), & \gamma_{\min} \geq 7.2 \end{cases} \tag{4}$$

where $\lambda$ is a negative constant, the $\mu$ is a positive constant, and its size is adjusted in time according to different working conditions and different actual projects. In order to ensure the normal commutation process, the extinction angle $\gamma$ needs to be greater than the minimum extinction angle $\gamma_0$, while $\gamma_0$ in practical engineering generally takes 7.2°. The reward function demonstrates that if the minimum extinction angle after the first commutation failure is still less than 7.2° after the parameter optimization, it indicates that the parameter is invalid and the reward function is negative; If the minimum extinction angle after the first commutation failure is greater than 7.2° after the parameter optimization, it indicates that the parameter is valid, furthermore the larger the minimum extinction angle is, the greater the reward function value is. By increasing the reward value, the required optimization parameters are obtained.

The training process diagram is shown below.

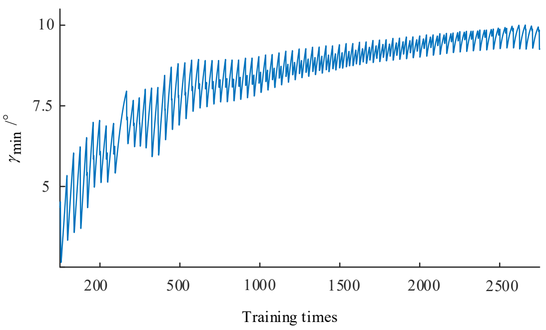


(a) Minimum of extinction angle

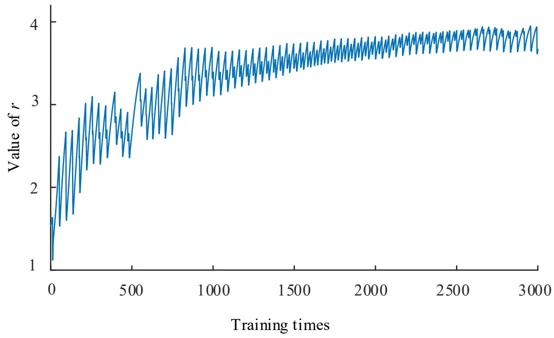


(b) Value of $r$ function

Fig. 6. Customized module of improved CEC

As shown in Fig. 6, the initial stage of the agent has poor control performance and a large oscillation amplitude of the output data. With the increase of the number of trainings and cumulative samples, the amplitude of the output data gradually converges, the minimum CEA gradually increases, the value of the reward function gradually increases, and the performance trend of the agent is good.

Finally, through the optimization results, it is determined that the optimal parameters of the CEC ramp function in this fault case should be: input_max=0.05 and output_max=0.31.

Based on the optimization results, an improved CEC method is proposed, and Fig. 7 shows the characteristic curve of the proposed CEC method.

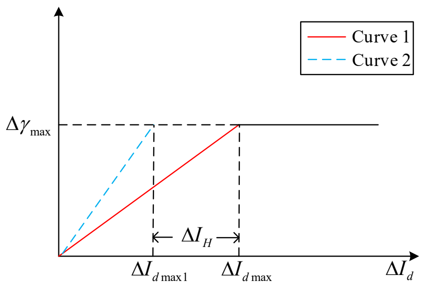


Fig. 7. Characteristic curve of adaptive current deviation control

When the system is operating normally, the CEC characteristic curve is curve 1; When the inverter-side control is switched to the CC control mode, the CEC uses offline optimized parameters to change the slope of the ramp function, so the characteristic curve changes to curve 2. At this time, the output of the CEC session will increase, accelerating the switching from CC control to CEA control and increasing the margin of the advanced trigger angle. The proposed control block diagram of the improved CEC method is shown in Fig. 8.

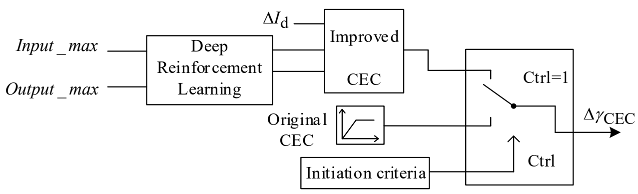


Fig. 8. Improved CEC control strategy

The starting criterion in Fig. 8 is: when "$\beta_C$>$\beta_G$" is detected, it is put into operation, and when "$\beta_C$≤$\beta_G$" is detected, the controller is back off. It can be ensured that the control strategy only works when the inverter is under CC control, reducing the impact of increasing the CEC slope on system recovery. Fig. 9 shows the simulation curve of the CEC output increment comparison of the two control strategies, and the CEC output increment can be increased by increasing the CEC slope, which is in line with the expected effect.

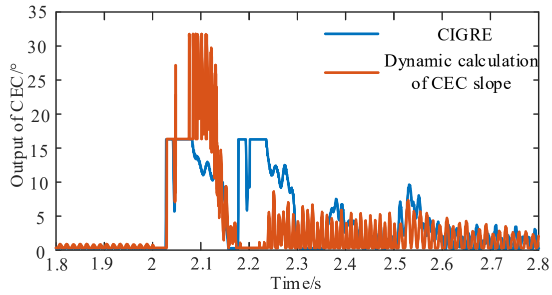


Fig. 9. Simulation comparison of extinction angle increment under two control strategies

## IV. Example Analysis

In this paper, the single-phase grounding fault or three-phase grounding fault of the AC transmission line in the actual project is simulated by the inductive grounding at the converter bus, and the severity of the fault is simulated by changing the size of the grounding inductor. The following is a simulation verification by two different control strategies.

Strategy 1: CIGRE standard test model control.

Strategy 2: On the basis of strategy 1, replace the CEC in the inverter-side DC control system to the control strategy proposed.

### *A. System Recovery Performance Vertification*

The three-phase grounding fault is set at 2s on the AC bus of the inverter, the ground inductance $L_f$ equals to 1H, the fault lasts for 0.5s, and the electrical quantity simulation response characteristics are shown in Fig. 10.

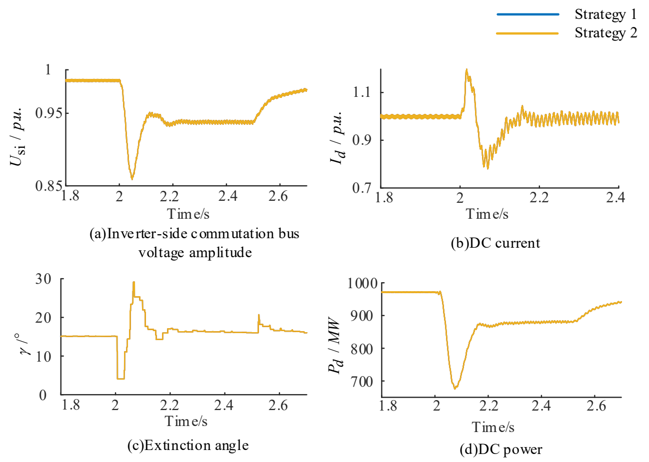


Fig. 10. System recovery characteristics under three-phase grounding fault ($L_f$=1H)

The fault is equivalent to the actual project of the slight AC fault. From Fig. 10 can be seen, under the fault condition, the DC system does not occur subsequent commutation failure, meanwhile, the strategy 2 and strategy 1 system recovery characteristics are highly consistent, which indicate that the control strategy proposed in the paper is started only when the system has the risk of subsequent commutation failure; otherwise, it does not start when the system has the slight fault. It proves that the start criterion of the control strategy proposed in this article is accurate and reasonable, and will not affect the fault recovery ability of the DC system.

### *B. Validation of Improved CEC Control Effect under Single-Phase Ground*

The single-phase ground fault is set at 2s on the AC bus of the inverter station, the ground inductance $L_f$ equals to 0.45H, the fault is cleared after 0.5s, and the electrical quantity simulation response characteristics are shown in Fig. 11.

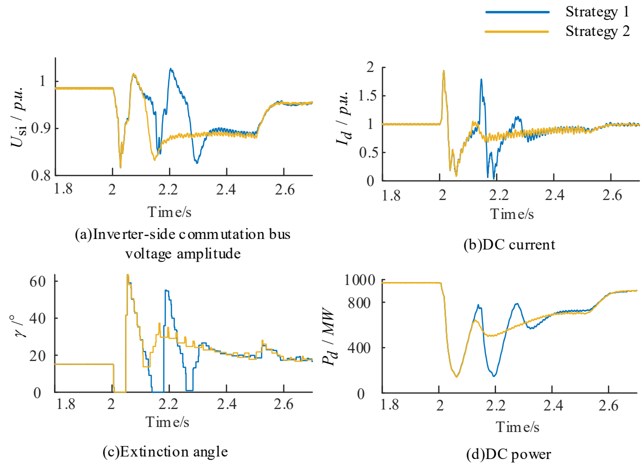


Fig. 11. System recovery characteristics under single-phase grounding fault ($L_f$=0.5H)

As can be seen from Fig. 11, control strategy 2 can effectively increase the extinction angle margin during the fault, improve the system recovery performance, and enhance the ability of the system to resist subsequent commutation failures.

### *C. Verification of the Effect of Improved CEC Method to Suppress Subsequent Commutation Failure*

In order to further verify the inhibition effect of the proposed control strategy on subsequent commutation failures, it is necessary to set up more AC faults of different severities for simulation experiments. The failure level $F_L$ is defined as follows [10]:

$$F_L = \frac{U_L^2}{L_f P_N} \times 100\% \tag{5}$$

where $P_N$ is the DC rated power.

The single-phase AC faults and three-phase AC faults with different severities between 5% and 50% of the fault level $F_L$ are simulated, and the number of commutation failures in the DC system is shown in Table I.

TABLE I. Commutation Failure Times in Different Control Strategies

| **Fault level/%** | **Strategy 1** | | **Strategy 2** | |
|---|---|---|---|---|
| | ***Single-phase fault*** | ***Three-phase fault*** | ***Single-phase fault*** | ***Three-phase fault*** |
| 5 | 0 | 0 | 0 | 0 |
| 10 | 0 | 0 | 0 | 0 |
| 15 | 0 | 2 | 0 | 1 |
| 20 | 2 | 2 | 1 | 1 |
| 25 | 2 | 2 | 1 | 1 |
| 30 | 3 | 2 | 1 | 1 |

| | | | | |
|---|---|---|---|---|
| 35 | 3 | 2 | 1 | 1 |
| 40 | 3 | 2 | 1 | 1 |
| 45 | 3 | 2 | 1 | 1 |
| 50 | 3 | 2 | 1 | 1 |

As can be seen from Table I, for different severities and different types of faults, strategy 2 can effectively suppress the occurrence of subsequent commutation failures of DC system.

## V. CONCLUSION

In this paper, by analyzing the influence mechanism of CEC on subsequent commutation failures, it is found that increasing the slope of the CEC ramp function can speed up the inverter side control mode switching, thereby shortening the fault recovery process, so a subsequent commutation failure suppression method based on deep reinforcement learning optimization of CEC parameters is proposed. Through simulation verification and analysis, the following conclusions are drawn:

*1)* When the inverter side control mode is under CC control, the switching angle of the inverter side is not controlled, and the risk of subsequent commutation failure increases; Increasing the slope of the CEC ramp function can improve the margin of the CEA during fault recovery, and can suppress the occurrence of subsequent commutation failures to a certain extent.

*2)* Based on the optimization model of deep reinforcement learning, the parameters in different system operating states can be optimized in the offline state, which enhances the ability of the system to resist subsequent commutation failures when running online.

## REFERENCES


[1] He Yangyang, Zheng Xiaodong, Tai Nengling, et al. A review of modeling methods for LCC-HVDC converter in AC/DC hybrid power grid[J]. Proceedings of the CSEE, 2019, 39(11): 3119-3130(in Chinese).

[2] Li Mingjie. Characteristic analysis and operational control of large-scale hybrid UHV AC/DC power grids[J]. Power System Technology, 2016, 40(04): 985-991(in Chinese).

[3] Song Jinzhao, Li Yongli, Zeng Liang, et al. A review of commutation failure for LCC-HVDC[J]. Automation of Electric Power Systems, 2020, 44(22): 2-13(in Chinese).

[4] Liu Lei, Lin Sheng, Liu Jian, et al. Mechanism analysis of subsequent commutation failures caused by improper interaction of controllers[J]. Power System Technology, 2019, 43(10): 3562-3568(in Chinese).

[5] Xia Haitao, Zhou Xiaoping, Hong Lerong, et al. An adaptive current deviation control method for suppressing following commutation failures[J]. Proceedings of the CSEE, 2019, 39(15): 4345-4356(in Chinese).

[6] Dai Zhihui, Pan Xingyu, Wang jingyu. Continuous commutation failure suppression method based on dynamic current deviation control[J]. Proceedings of the CSU-EPSA, 2021, 33(03): 49-58(in Chinese).

[7] Song Xinfu, Chen Weiwei, Zhou Bohao, et al. Influence of current error controller on commutation failures and system recovery[J]. Electric Power Engineering Technology, 2022, 41(02): 37-44(in Chinese).

[8] Li Zhixian, Li Huan, Liu Chongru, et al. State-space model and solution algorithm of an HVDC system considering a snubber circuit[J]. Power System Protection and Control, 2022, 50(11): 91-101(in Chinese).

[9] S. Tamai, H. Naitoh, F. Ishiguro, et al. Fast and predictive HVDC extinction angle control[J]. IEEE Transactions on Power Systems, 1997, 12(3): 1268-1275.

[10] Cong Xinpeng, Zheng Xiaodong, Cao Yaqian, et al. A suppression strategy for subsequent commutation failures considering commutation capability of recovery process[J]. Journal of Shanghai Jiaotong University, 2022, 56(03): 333-341(in Chinese).